New Experimental Results on Dynamic Biot Coefficient on Brazilian Reservoir Rocks

Guilherme F. Vasquez, Márcio J. Morschbaher, Julio C. R. Justen (Petrobras), and Ana Júlia P. P. M. Silveira (Fundação Gorceix)

This paper was prepared for presentation during the 14th International Congress of the Brazilian Geophysical Society held in Rio de Janeiro, Brazil, August 3-6, 2015.

Abstract

Predicting or estimating pore pressure from seismic data is a common goal on exploration and reservoir geophysics. In exploration there is the important issue of abnormal pore pressure prediction in order to assist on a better well drilling program, avoiding unnecessary costs and also dangerous hazards associated to unexpected high pore pressure zones. During the production phase, time lapse seismic interpretation may help to improve and update the reservoir model if one can estimate both pore pressures and saturation changes from 4D data.

The use of seismic data or acoustic well logs to estimate pore pressure relies essentially on the fact that the seismic-wave velocities are sensitive to the effective stress. Generally the effective stress is assumed to be the difference between overburden stresses and pore pressure, as a first approximation. This is a good approximation for loose sands and other unconsolidated reservoirs, but may fail even in weakly cemented rocks. A more refined approach is to use the Biot coefficient, or an effective stress coefficient, as a weighting parameter multiplying the pore pressure, so that the effective stress is the overburden stress minus this coefficient times the pore pressure.

In this paper we present new results on the measurement of the dynamic Biot coefficient of Brazilian rocks based on the method introduced by Todd and Simmons (1972). We interpret and discuss the results in terms of rock texture and compare it to some previous results obtained on the past.

Introduction

Abnormal pore pressure prediction is a crucial issue on exploratory wells drilling, especially in new areas. It may avoid unnecessary costs in well planning if there is no need of related turnarounds, and it may prevent undesirable accidents that may lead to well, material or even life losses.

During the exploitation phase the pore pressure estimation is still desirable in order to help new well planning and production strategies, because it may reveal unexpected compartmentalization on the reservoir.

The prediction of abnormal pore pressures based on exploratory seismic data generally uses methods based on Eaton formulation (Dutta, 2002). On the other hand, in time-lapse seismic data analysis, there are at least two data sets and some a priori pore pressure information, but one may take into account changes in reservoir pressure as well as in saturation (Landrø *et al*., 2003). In both exploration and production, the pore pressure prediction relies on the fact that the seismic-wave velocities are sensitive to the effective stress acting on the rocks. Although the effective stress is a tensor, for the sake of simplicity this paper will consider only the isotropic stress case, in which we can deal with stress as a scalar quantity.

As a first approximation we can replace the effective stress P_{ef} by the differential stress,

$$P_d = P_c - P_p, \tag{1}$$

were P_c is the confining stress (or overburden stress, on the field) and P_p is the pore pressure. This is an excellent approximation in soil mechanics, as in the case of Terzaghi's principle, and even for real reservoirs composed of permeable and porous rocks.

A more precise approach may include a weighting factor multiplying the pore pressure, so that

$$P_e = P_c - n\,P_p. \tag{2}$$

This factor is generally assumed as the Biot coefficient (*cf.* Biot and Willis, 1957). In fact, Nur and Byerlee (1971) had shown that, for a bulk compression of a porous media, the Biot coefficient

$$\alpha = 1 - \frac{K_d}{K_m} \tag{3}$$

is the correct weighting factor for the pore pressure. In other words, the bulk modulus of the saturated porous material, K, depends only on the difference

$$P_c - \alpha\,P_p \tag{4}$$

The only requisite is that the solid part is elastic. Nevertheless, Berrymann (1993) shows that, for different properties of a multicomponent porous media, different weighting factors must be used.

Todd and Simmons (1972) suggest a method for evaluating the weighting factor for compressional-wave velocity. They suggest naming this weighting factor as the empirical Biot coefficient, but other authors call it effective stress coefficient (for velocity) or dynamic Biot coefficient (Yu, 2015).

Since then, some authors also derived the dynamic Biot coefficient for compressional and shear-wave velocities based on Todd and Simmons' method. There are even results on similar rocks, from the same geological formation, derived by different authors (e.g. Berea Sandstone and other "famous" outcrop rocks).

In general it is observed that the effective stress coefficient is less than one. It is quite low for low porosity rocks, and tends to one as the porosity increases. Some authors show that the coefficient depends also on the effective stress and pore pressure, and suggests a method of minimizing the fluid incompressibility effect on the calculation (*cf*. Vasquez *et al*., 2008).

We present new results on the dynamic Biot coefficient for Brazilian reservoir rocks. The results are interpreted and compared to old results obtained by our team as well as from other authors.

Method

The method to infer the dynamic Biot coefficient is based on Todd and Simmons (1972) pioneering work. They had shown that the compressional-wave velocity depends on the effective pressure $P_e = P_c - n\,P_p$ were the factor n is given by

$$n = 1 - \frac{\left(\frac{\partial V_p}{\partial P_p}\right)_{P_d}}{\left(\frac{\partial V_p}{\partial P_d}\right)_{P_p}} \qquad (5)$$

Based on this result, it is possible to obtain the partial derivatives of compressional-wave velocity relatively to pore pressure and differential pressure though the use of several velocity measurements as a function of confining pressure, with different pore pressures, as illustrated on the scheme of Figure 1.

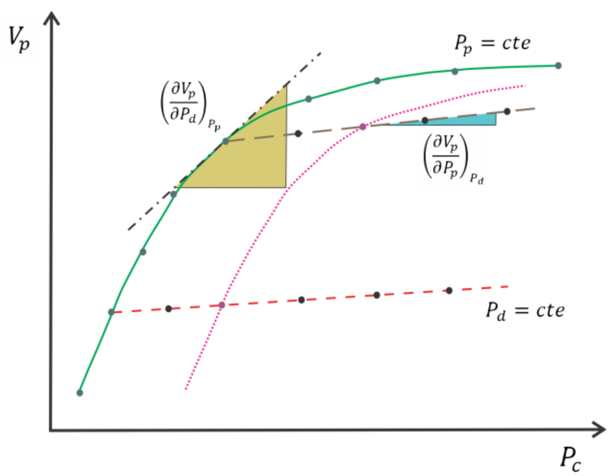

Figure 1: *Schematic diagram of velocity versus confining pressure with the necessary partial derivatives for applying Todd and Simmons' method. The continuous green curve correspond to velocity measurements obtained at different confining pressures with a particular pore pressure value, and the dotted pink curve to another pore pressure value. The dashed orange and brown straight lines correspond to velocity data collected at two particular differential pressure values.*

The velocity curve for a constant differential stress is a straight line. If the line is perfectly horizontal, $n = 1$, while for velocity increasing with confining pressure for a constant differential pressure, $n < 1$. It must be noted that there are some results on the literature which found coefficients such that $n > 1$, corresponding to velocity decreasing with increasing confining pressure for constant differential pressure.

At first glance it may sound strange that any rock exhibits $n > 1$, but it only means that the role of pore pressure on velocity behavior is prominent compared to that of the confining pressure. It must be kept in mind that the effective stress coefficient or dynamic Biot coefficient is not necessarily equal to the "classic" Biot coefficient, defined by Equation (3), which is always less or equal to one.

The compressional and shear-wave velocities were measured by the ultrasonic pulse transmission technique, varying the confining stress along increasing and decreasing stress paths with constant pore pressures. Theoretically the velocity would not depend on the stress path. Some tests were made to check the occurrence of hysteresis or dependence on the stress path and in fact it is negligible.

In order to obtain the partial derivative of velocity relatively to differential stress $(\partial V/\partial P_d)_{P_p}$ the velocity data at each constant pore pressure was adjusted by fitting a function of the form

$$V(P_d) = a - b \times exp(-P_d/c) \qquad (6)$$

and to obtain the partial derivative $\left(\partial V/\partial P_p\right)_{P_d}$ linear functions were fitted to the velocity data at each differential stress value.

The choice of the particular function represented by Equation (6) is somewhat arbitrary, since there are a number of functions commonly used to mimic the velocity behavior as a function of effective stress (Vasquez *et al*., 2005). This particular function has the advantage to reach an asymptotic value at very high stresses.

The samples were saturated with alcohol (ethanol) to avoid interaction between pore fluid and solids, like clay swelling on the sandstone due to water or shear weakening in the limestone, as observed by many authors (e.g.: Bathija *et al*., 2009; Baechle *et al*., 2009; Vanorio *et al*., 2008; Morschbacher *et al*., 2015). Another reason to use ethanol as the saturating pore fluid relies on the fact that its bulk modulus and density is similar to those of some typical live oils, as noted by Vasquez, 2009.

It must be noted that the original in situ effective stress is different for each one of the reservoirs, and this value was adopted as the ultimate differential stress on the laboratory tests. For the sandstone reservoir the confining pressures assumed values from 1000 up to 14000 PSI (6.89 up to 96.53 MPa) and pore pressures from atmosphere up to 10000 PSI (68.95 MPa) at 1000 PSI (6.89 MPa) steps. For the carbonate reservoir the confining stress used were from 5 up to 50 MPa (725 up to 7251 PSI) and pore pressure from atmosphere up to 45 MPa (6527 PSI).

Rock Sample Characteristics

Two different Brazilian offshore reservoirs from deep water Santos Basin were used in this study.

The first reservoir is composed by consolidated sands, low to medium porosity and low to moderate permeability. These are well consolidated arcosic sandstones, with more than 50% feldspar on average, fine to medium grained, poorly to moderately sorted, and relatively rich in chlorite, especially as fringes or coatings around the grains. The porosity of these sandstones includes micro porosity associated with the chlorite. Figure 2 displays a typical Scanning Electron Microscopy (SEM) photography of this sandstone where one can note the chlorite coating on the grains. The fringes may be noted also on the thin section photography shown on Figure 3 as a further illustration of the sand characteristics.

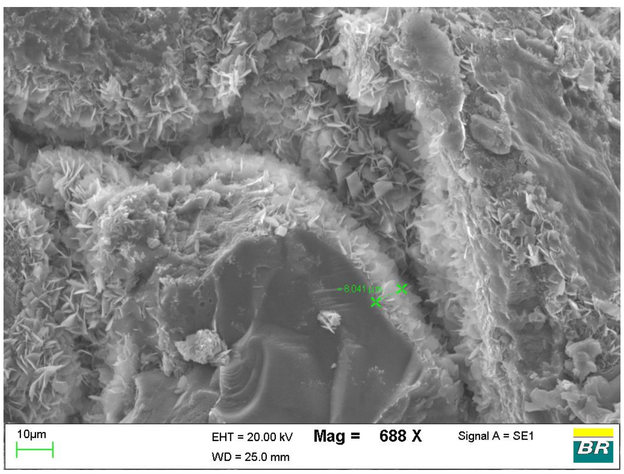

Figure 2: *SEM photography of one sandstone sample. Note the chlorite coating on the grain surface. This coating contains non-negligible micro porosity.*

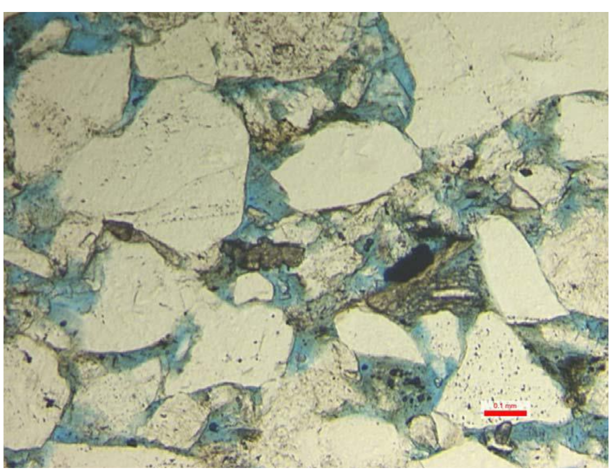

Figure 3: *Thin section photography of one of the sandstone facies, a fine grained, moderately sorted sandstone, with intergranular and fringe clay (chlorite), with some preserved porosity.*

The other reservoir used on this study is a carbonate reservoir. This is mainly a limestone reservoir with widely varying texture, from mudstone to rudstone, whilst the better reservoir facies are grainstones and rudstones. There is eventually small amount of silica and dolomite in some reservoir intervals, associated with early diagenetic events. Generally these secondary minerals do not damage the reservoir quality, occurring more associated to mineral substitution than deposition on pore space. Most part of the samples used may be classified as grainstones and rudstones. Figure 4 illustrates a thin section photography of one of the samples, in this case a high porosity rudstone which solid components are rich in shells.

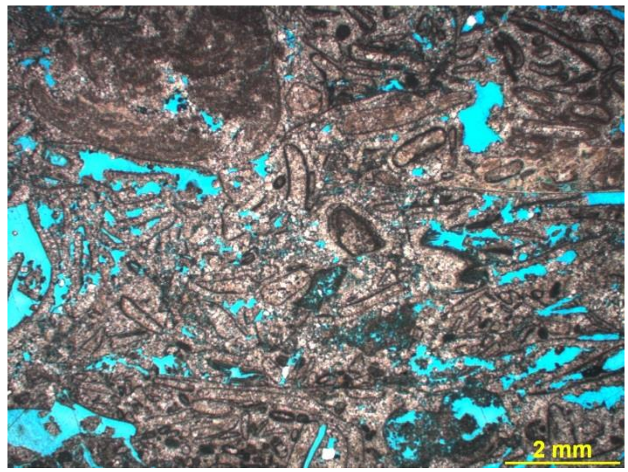

Figure 4: *Thin section photography of one of the limestone samples used on this study, a rudstone rich in shells with some peloidal particles and high porosity.*

Results

Some examples from each reservoir rock are presented here to illustrate our results.

Figure 5 displays a scatter diagram for the compressional-wave velocity as a function of confining stress for one of the sandstone samples, with 16.7% porosity and 15.2 md permeability. Only two constant pore-pressure curves and two constant differential stresses are shown for simplicity. From the slope of the constant differential stress lines it is evident that the coefficient n will be smaller than one, since the velocity increases with increasing confining stress for constant differential stress. The corresponding empirical Biot coefficients for P-wave velocity are shown on Figure 6 as a function of differential stress. Each different symbol corresponds to a particular pore pressure value.

In general, the empirical Biot coefficient n decreases with increasing differential stress and, for each differential stress, the coefficient decreases with increasing pore pressure. It is interesting to note that the behavior is monotonic and smooth. For high differential stresses the coefficient can be as low as 0.6 for low pore pressures and even below 0.4 for high pore pressure.

There are some discussion on literature regarding the uncertainty on n estimation for high confining and differential stress (Vasquez *et al*., 2010). On the other hand, one should expect that at very high confining stresses the rock moduli are so high that the fluid pressure may play a minor role on elastic-wave velocities.

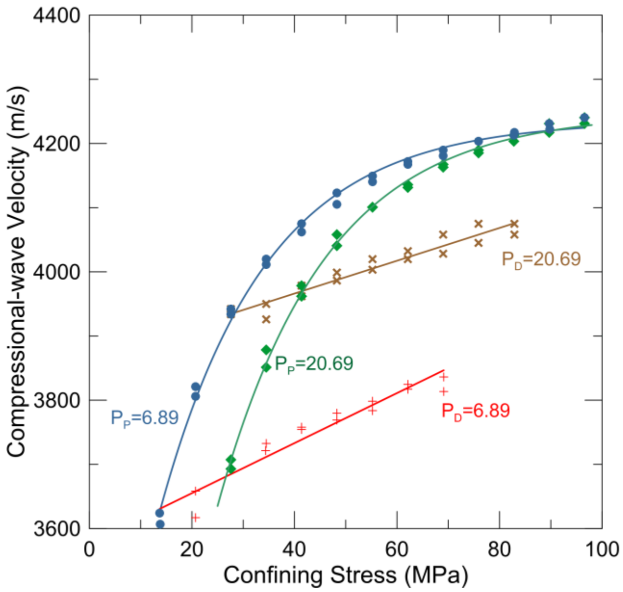

Figure 5: *Example of compressional-wave velocity results for an arcosic sandstone sample a function of confining pressure with some constant pore pressure and constant differential pressure curves.*

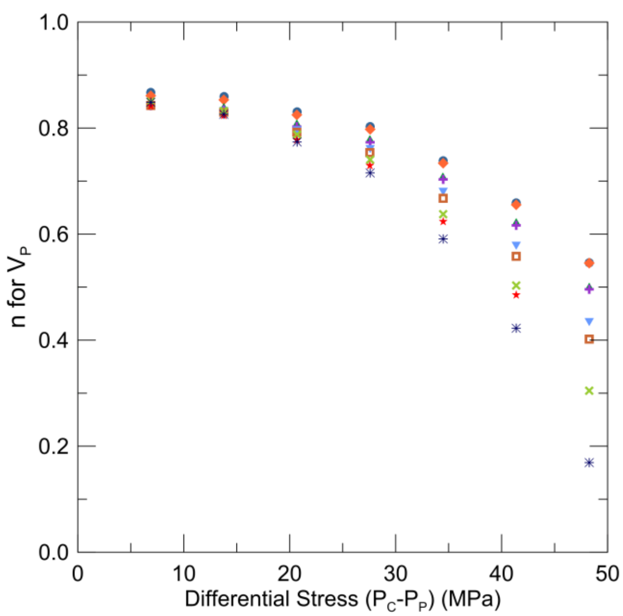

Figure 6: *Example of empirical Biot coefficient for P-wave velocity for a sandstone sample as a function of differential pressure. Different symbols correspond to different pore pressures. In general, for a given differential stress, n decreases with increasing pore pressure.*

The observed behavior for the empirical Biot coefficient for the sandstone samples is very reasonable, and agrees with other measurements made on similar sandstones (Vasquez *et al*., 2008).

An example of P-wave velocity behavior as a function of differential stress for the carbonate reservoir is shown on Figure 7. The particular sample illustrated here has 21.1% porosity and 254 md permeability. The corresponding dynamic Biot coefficients are shown on Figure 8.

Note that the values for the empirical Biot coefficient n are higher than those obtained for the sandstone sample. The coefficient n decreases with increasing differential stress as in the sandstone case, decreasing with increasing pore pressure as well.

It must be kept in mind that the scales for figures 7 and 8 are different from those on figures 5 and 6, because we had limitations on the ultimate pressures due to the original in situ effective stress acting on the reservoirs, since we must avoid unnecessary mechanical damage of rock samples.

The observed behavior for the dynamic Biot coefficient of the limestone samples is not as smooth as on the case of the sandstones. There is a suspicion that this not so regular behavior is associated to the poor waveform quality obtained on the limestone cores. Some samples presents large vugs and grains that may even cause "patchy dispersion", causing waveform distortion and impairing a good first arrival picking (*cf*. Zinszner and Pellerin, 2007).

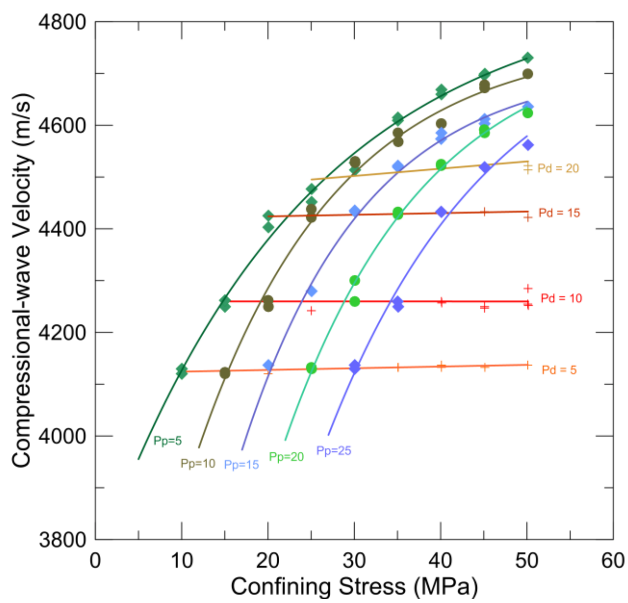

Figure 7: *Example of compressional-wave velocity results for a limestone sample (rudstone) as a function of confining stress with some constant pore pressure and constant differential stress curves.*

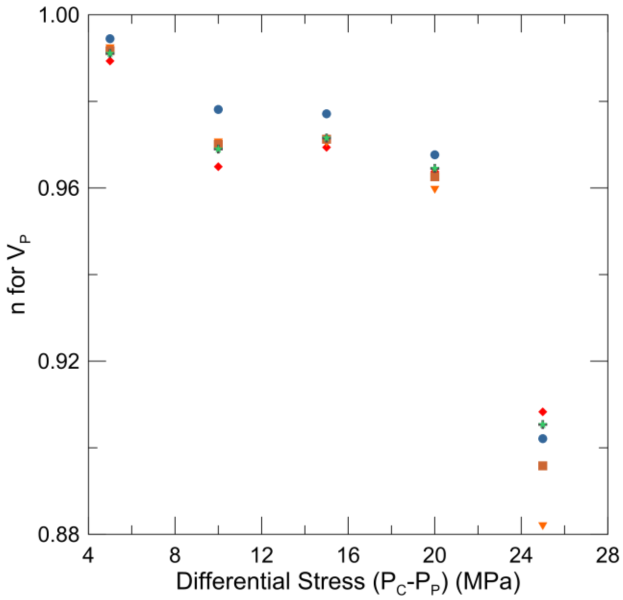

Figure 8: *Example of empirical Biot coefficient n for P-wave velocity for a rudstone limestone sample as a function of differential stress. Different symbols correspond to different pore pressures values. In general, for a given differential stress, the coefficient decreases with increasing pore pressure.*

Figures 9 illustrate the compressional and shear waveforms recorded for one sandstone sample and one limestone sample at similar confining stress and pore pressure conditions. Note that, in this figure, the waveform quality is not so poor because the differential stress is high (around 40 MPa), but it is clear that the sandstone presents clearer waveforms when compared to the limestone. At lower differential stresses it is quite difficult to identify the shear-wave first arrival due to the waveform distortions.

As general remarks, it was observed that the consolidated sandstone reservoir presented dynamic Biot coefficients n bellow 0.9. On the other hand, the limestone reservoir, although it is also comprised by well consolidated rocks, presented Biot coefficients above 0.9 for low differential stresses. In both cases (sandstones and limestones) there is a clear decreasing trend of the n coefficient with increasing differential stress, as wells as with increasing pore pressure, for a fixed differential stress.

These differences in the dynamic Biot coefficient ranges for the different reservoir rocks may be related not only to the porosity values, but also to the pore space geometry. Although several authors suggest this relationship among Biot coefficient and pore geometry, the comprehension of the phenomena is not so straightforward (*cf.* Prasad and Maghnani, 1997; Xu *et al*., 2006). Qualitatively, the consolidated sandstone seems to have poorer pore communication when compared to the limestone rocks. The chlorite coating may exaggerate even more this situation.

These results are coherent with previous results obtained on Brazilian reservoir rocks (Vasquez *et al*., 2010).

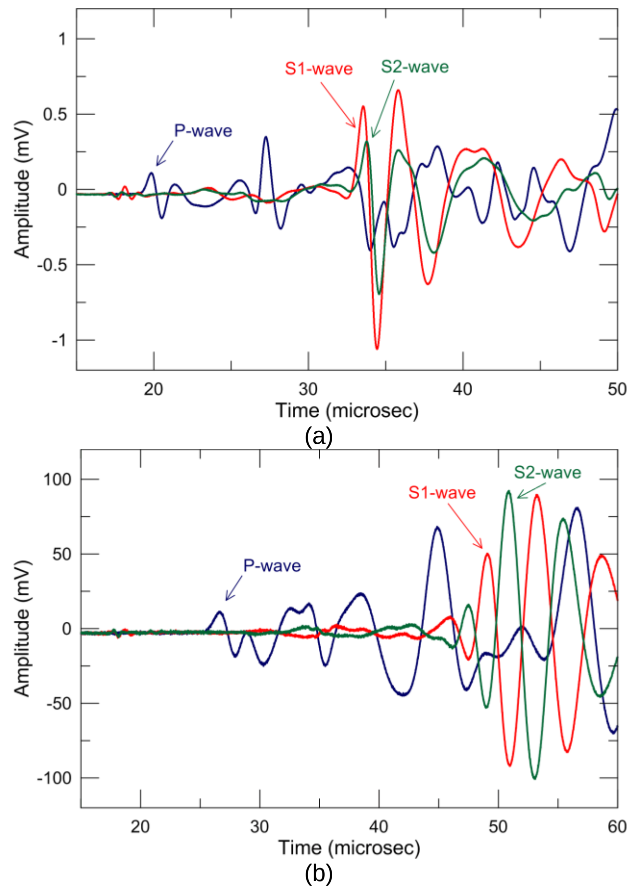

Figure 9: *Waveforms recorded for a sandstone sample (a) and a limestone sample (b) samples similar confining stress and pore pressure conditions. Note that, as these waves corresponds to high effective stress (near 40 MPa), the waveform quality is reasonably good even for the limestone. Nevertheless, the waveform quality for the sandstone is much better than for the limestone, especially for the shear waves. At lower differential stresses the quality is usually worst. The amplitude value may not be compared among the two different rocks because there was distinct external gains and source energy applied.*

Conclusions

New results of empirical Biot coefficient, or effective stress coefficient n related to elastic-wave velocities for Brazilian reservoir rocks were presented.

These new results agree with the initial expectation: the coefficient tends to decrease with increasing differential stress and pore pressure. The coefficient also increases with increasing porosity.

The dynamic Biot coefficient found for the sandstone and limestone reservoirs agrees with previous results on similar rocks as well, although this carbonate reservoir is quite peculiar.

Acknowledgments

The authors thank Petrobras for the permission to publish this paper and the support on the research. We are in debt with our colleagues from the Rock Physics Lab at Petrobras' Research Center, as well as those from the Rock-Log-Seismic Integration Section, specially the Manager Vinicius Machado for encouraging this research.

References

Baechle, G.T., Gregor P. Eberli, G.P., Ralf J. Weger, R.J., and Massaferro, L. 2009. Changes in dynamic shear moduli of carbonate rocks with fluid substitution. *Geophysics*, V. 74, No. 3., pp. E135-E147

Bathija, A.P., Liang, H., Lu, N., Prasad, M., and Batzle, M.L. 2009. Stressed swelling clay. *Geophysics,* V. 74, No. 4, pp. A47-A52.

Berryman, J.G. 1993. Effective stress rules for pore-fluid transport in rocks containing two minerals. *Int. J. Rock Mech. Min. Sci. & Geomech. Abst*., V. 30, pp. 1165–1168.

Biot, M.A., and Willis, D.G. 1957. The elastic coefficients of the theory of consolidation. *Journal of Applied Mechanics*, ASME, 24, pp. 594–601.

Dutta, N.C. 2002. Geopressure prediction using seismic data: Current status and the road ahead. *Geophysics*, V. 67, No. 6, pp. 2012–2041.

Landrø, M., Veire, H.H., Duffautz, K., and Najjar, N. 2003. Discrimination between pressure and fluid saturation changes from marine multicomponent time-lapse seismic data. *Geophysics*, V. 68, No. 5, pp. 1592-1599.

Morschbacher, M.J., Vasquez, G.F., Justen, J.C.R., and Silveira, A.J.P.P.M., 2015. Implicações da interação rocha-fluido na geofísica de reservatórios carbonáticos. *14th International Congress of the Brazilian Geophysical Society*. Rio de Janeiro, Brazil, August 3-6, 2015. (Submitted).

Nur, A., and Byerlee, J.D. 1971. An exact effective stress law for elastic deformation of rocks with fluids. *Journal of Geophysical Research*, V. 76, pp. 6414–6419.

Prasad, M., and Manghnani, M. 1997. Effects of pore and differential pressure on compression wave velocity and quality factor in Berea and Michigan sandstones. *Geophysics*, V. 62, No. 4, pp. 1163–1176.

Todd, T., and Simmons, G. 1972. Effect of pore pressure on the velocity of compressional waves in low-porosity rocks. *Journal of Geophysical Research*, V.77, pp. 3731–3743.

Vanorio, T., Scotellaro, C., and Mavko, G. 2008. The effect of chemical and physical processes on the acoustic properties of carbonate rock. *The Leading Edge*, V. 27, No. 8, pp. 1040-1048.

Vasquez, G., Dillon, L., Justen, J., Nunes, C., and Bacelar, C. 2005. Dry Rock Elastic Moduli Behavior with Pressure. *9th International Congress of the Brazilian Geophysical Society* Expanded Abstracts. Salvador, Brazil, 11-14 September 2005.

Vasquez, G.F., Vargas Jr., E.A., Ribeiro, C.J.B., Leão, M., and Justen, J.C.R. 2008. Experimental determination of the effective pressure coefficients for Brazilian limestones and sandstones. *Revista Brasileira de Geofísica*, V. 27, No. 1, pp. 1-11.

Vasquez, 2009. *Influência das Condições Geomecânicas na Estimativa de Poropressões Baseada nas Respostas Sísmicas das Rochas*. DSc. Thesis, Universidade Federal do Rio de Janeiro.

Vasquez, G.F., Vargas Jr., E.A., Justen, J.C.R., and Morschbacher, M.J. 2010. How Effective Is the Effective Stress Coefficient – An Experimental Study on Brazilian Rocks. *72nd EAGE Conference and Exhibition incorporating SPE EUROPEC 2010. Barcelona, Spain, 2010*. Paper P355.

Xu, X., Hofmann, R., Batzle, M., and Tshering, T. 2006. Influence of pore pressure on velocity in low-porosity sandstone: Implications for time-lapse feasibility and pore-pressure study. *Geophysical Prospecting*, 54, pp. 565–573.

Yu. H., 2015. Dynamic effective pressure coefficient calibration. Geophysics, V. 80, No. 1., pp. D65-D73.

Zinszner, B., and Pellerin, F.M. 2007. *A Geoscientist's Guide to Petrophysics.* Editions Technip, Paris, France. 384 p. (cf. p. 231)